AGU ADVANCING EARTH AND SPACE SCIENCES

Geophysical Research Letters

RESEARCH LETTER
10.1029/2024GL109296

Key Points:

- The effects of future aerosol reductions in China due to achieving carbon neutrality on solar and wind energy are investigated
- Aerosol emission reductions, especially in eastern China, increase surface downwelling shortwave radiation, temperature and wind speed
- Climate changes resulting from emission reductions under carbon neutrality enhance the potential of solar and wind energy

Supporting Information:

Supporting Information may be found in the online version of this article.

Correspondence to:

Y. Yang,
yang.yang@nuist.edu.cn

Citation:

Ren, L., Yang, Y., Wang, H., Wang, P., Yue, X., & Liao, H. (2024). Co-benefits of mitigating aerosol pollution to future solar and wind energy in China toward carbon neutrality. *Geophysical Research Letters*, *51*, e2024GL109296. https://doi.org/10.1029/2024GL109296

Received 15 MAR 2024
Accepted 12 JUN 2024

Co-Benefits of Mitigating Aerosol Pollution to Future Solar and Wind Energy in China Toward Carbon Neutrality

Lili Ren[1,2,3], Yang Yang[2], Hailong Wang[4], Pinya Wang[2], Xu Yue[2], and Hong Liao[2]

[1]School of Environment and Ecology, Jiangsu Open University, Nanjing, Jiangsu, China, [2]Jiangsu Key Laboratory of Atmospheric Environment Monitoring and Pollution Control, Joint International Research Laboratory of Climate and Environment Change (ILCEC), Jiangsu Collaborative Innovation Center of Atmospheric Environment and Equipment Technology, School of Environmental Science and Engineering, Nanjing University of Information Science and Technology, Nanjing, Jiangsu, China, [3]Jiangsu Urban and Rural Water Environment Governance Low Carbon Development Engineering Technology Center for Ecological and Environmental Protection, Jiangsu, China, [4]Atmospheric, Climate, and Earth Sciences Division, Pacific Northwest National Laboratory, Richland, WA, USA

Abstract The climate commitment to achieving carbon neutrality before 2060 in China has been announced recently. In the context of pursuing carbon neutrality, sharing similar sources as greenhouse gases, aerosol particle and precursor emissions are projected to substantially decrease in China, which can potentially have a great impact on climate. Here, we investigate the effects of future aerosol reductions, because of achieving carbon neutrality, on solar and wind energy in China by using an earth system model. We show that significant reductions in aerosol emissions, particularly in eastern China, lead to increases in the surface downwelling shortwave radiation, surface air temperature and wind speed, which can further enhance the potential of solar and wind energy production. The findings underline that the pursuit of carbon neutrality can yield co-benefits of not only mitigating climate change and air pollution but also fortifying the stability of renewable energy sources.

Plain Language Summary In response to China's commitment to achieve carbon neutrality by 2060, our study examines the potential impact of reducing aerosol emissions and greenhouse gases on solar and wind energy generation. Employing an earth system model, we observe significant reductions in aerosols, particularly in eastern China, resulting in increases in surface downwelling shortwave radiation, surface air temperature, and wind speed. These changes have promising implications for enhancing solar and wind energy production. Our research underscores the interconnected benefits of pursuing carbon neutrality, encompassing climate change mitigation, air quality improvement, and the enhancement of renewable energy reliability.

1. Introduction

Carbon neutrality, which aims to achieve net-zero carbon dioxide emissions by balancing carbon emissions and carbon sinks, heavily relies on the reduction of carbon emissions as a primary pathway to accomplishing this goal (Huang & Zhai, 2021; Rogelj et al., 2021). The realization of carbon neutrality is crucial for curbing global warming as it helps to limit the rise in global temperatures and reduce the impacts of extreme weather events and climate change. To keep global warming below 1.5°C above the pre-industrial levels, carbon neutrality needs to be achieved by the middle of the 21st century. In September 2020, China announced its plan to reach peak CO_2 emissions by 2030 and achieve carbon neutrality by 2060 (P. Wang et al., 2023; H. Yang et al., 2022; Zhao, 2022). As the world's largest energy consumer and CO_2 emitter, China's efforts in reducing CO_2 emissions will make an unparalleled contribution to mitigating global climate change (Z. Liu et al., 2022; Y. Yang et al., 2023). To attain the carbon neutrality goal, China has already implemented a series of climate policies and regional clean air measures, aimed at reducing fossil fuel burning emissions, including short-lived aerosols and precursors (Shindell & Smith, 2019). Accelerating the global journey toward carbon neutrality requires countries to strengthen their emission reduction efforts and actively promote the transition to renewable energy.

Solar and wind energy are two critical forms of renewable energy that are gaining increasing global attention (Y. Chen et al., 2023; Lei et al., 2023). As both energy demand and concern about climate change continue to grow, the utilization of these clean energy sources becomes ever more significant. Solar photovoltaic (PV) power generation converts incoming solar energy at the surface into electricity using photovoltaic cells. It mainly relies on solar irradiance and other atmospheric variables that affect the efficiency of the photovoltaic cells, such as surface air temperature and wind velocity (AlSkaif et al., 2020; Feron et al., 2021). Conversely, wind energy generation is highly dependent on wind speed. Fluctuations in wind speed and meteorological conditions can significantly impact the reliability and stability of wind energy production (M. Gao et al., 2018; Pryor & Barthelmie, 2011). To fully utilize the potential of solar energy and wind energy, it is imperative to make informative predictions and strategic plans considering meteorological conditions. Understanding and adapting to the meteorological dependence of these renewable energy sources are of great importance, especially in the context of climate change.

Many studies have investigated the impact of climate change on solar and wind energy generation. Using high-resolution climate models from Coordinated Regional Downscaling Experiment (CORDEX-AFRICA), Bichet et al. (2019) found that a decline in solar radiation and an increase in surface air temperature were expected to result in an average decrease of 4% in the annual mean solar potential over most of Africa by the end of the 21st century under the climate scenario Representative Concentration Pathway (RCP) 8.5. Park et al. (2022) projected the solar energy resource over East Asia to decrease by −4.3% (winter) to −1.5% (summer) under the RCP 8.5 scenario. Sailor et al. (2008) focused on the wind power generation potential in five states of the northwest United States (Idaho, Montana, Oregon, Washington, and Wyoming), comparing the 20th century baseline simulations with future climate scenarios from the Special Report on Emissions Scenarios (SRES A1B and A2). They found that summer wind speeds in the region might decline by 5%–10%, resulting in a potential 40% reduction in summertime wind power generation due to climate change. L. Chen (2020) explored future changes in wind resources across North America by analyzing high-resolution simulation data from the North America downscaling project (NA-CORDEX). Their findings indicated a projected decrease in wind power over the western United States and the East Coast by the end of the 21st century under the RCP 8.5 scenario, while the Southern Plains are expected to experience a substantial increase in wind power during spring and summer, with potential gains reaching up to 20%.

Given the context of actively pursuing carbon neutrality goals, aerosols reductions could potentially influence weather and climate, subsequently affecting solar and wind energy generation. In our previous study, the global impacts of changing greenhouse gases (GHGs), aerosols, and tropospheric ozone (O_3) following a carbon neutrality pathway on climate and extreme weather events were individually assessed using the Community Earth System Model version 1 (CESM1) (P. Wang et al., 2023). The results suggest that future aerosol reductions significantly contribute to climate warming and increase the frequency and intensity of extreme weather events, and aerosol impacts far outweigh those of GHGs and tropospheric O_3. Through an in-depth exploration of this issue, our objective is to uncover how the reduction in aerosols might affect the potential and variability of solar and wind energy. To comprehensively address this issue, we conduct Earth system model experiments to assess the impact of aerosols reductions on variables such as solar radiation, surface temperature, and wind speed, as well as their implications for energy generation potential. Our aim is to provide valuable insights to guide the establishment of sustainable energy planning and strategies in China's pursuit of carbon neutrality.

2. Methods

2.1. Model Description and Experimental Design

This study investigates the changes in solar and wind energy potentials under the carbon neutrality scenario using the fully coupled CESM version 1.2.2 (CESM1, Hurrell et al., 2013). The atmospheric component, the Community Atmosphere Model version 5 (CAM5), is employed to simulate major aerosol species, including sulfate, black carbon (BC), primary organic aerosol, and secondary organic aerosol. These aerosol components are categorized into four lognormal size distribution modes: Aitken, accumulation, coarse, and primary carbon modes (X. Liu et al., 2016). The model is configured with a horizontal resolution of 2.5° longitude by 1.9° latitude and 30 vertical layers. Aerosol particles within each mode exhibit an internal mixing state, while particles from different modes are externally mixed. The model explicitly considered aerosol radiative effects, encompassing both aerosol-radiation interactions and aerosol-cloud interactions (ACI) for stratiform clouds. In our study, we specifically improved the CESM model by introducing a new unified scheme for convective transport and aerosol wet removal with explicit aerosol activation above convective cloud base. This new implementation reduces the excessive BC aloft to better simulate observed BC profiles that show decreasing mixing ratios in the mid-to upper-troposphere. Additionally, these improvements also resulted in better Aerosol Optical Depth (AOD) over various global regions when compared to multi-year AERONET retrievals (H. Wang et al., 2013). For the scenario of achieving carbon neutrality in China, we utilize the DPEC (Dynamic Projection for Emissions in China) model-projected emissions, which take socio-economic development, climate policies, and pollution control measures into account, to acquire emissions anthropogenic aerosols and precursor gases during the carbon neutrality period (Y. Cheng et al., 2021; Tong et al., 2020). In comparison to the commonly used Shared Socioeconomic Pathways scenarios for global future climate simulations, the DPEC scenarios comprehensively consider local policies and effectively capture the rapid declining trends of $PM_{2.5}$ levels in China after 2015 (Y. Cheng et al., 2021). What's more, with the effects of current-year bias and inadequate considerations of pollution control policies, $PM_{2.5}$ projections in 2050 with CMIP6 mitigation scenarios are 59%–73% (8–12 μg/m^3) higher than projections with DEPC. Aerosols and precursor emissions from outside China and global greenhouse gas concentrations are obtained from CMIP6 (Coupled Model Intercomparison Project Phase 6) data and are locked at year-2015 levels for all experiments.

Fully-coupled experiments are conducted to examine the climate impacts of emission changes of anthropogenic aerosols in China under the "Carbon-Neutral" scenario in 2060 from the DPEC model (Table S1 in Supporting Information S1). Additionally, a baseline simulation is performed, with emissions in China also set at year-2015 levels, serving as the reference experiment. To minimize the influence of natural variability in the climate system, three initial-condition ensemble members are carried out for all experiments (Ren et al., 2022; Y. Yang et al., 2020). Each ensemble member is integrated for 70 years, with the first 20 years treated as model spin-up and the subsequent 50-year averages used for analysis. Apart from the coupled atmosphere-ocean configuration, we also conduct a set of atmosphere-only experiments driven by prescribed present-day monthly sea surface temperatures and sea ice concentrations to estimate effective radiative forcing (ERF) of aerosols (Ghan, 2013). Other configurations remain consistent with the coupled experiments. The horizontal winds in the atmosphere-only experiments are nudged toward MERRA-2 reanalysis under present-day conditions, facilitating the ERF estimation in short time periods. These atmosphere-only experiments are integrated for 10 years, with the averages of the last 9 years utilized for ERF estimation.

2.2. Estimating the Power Generation Potential

The PV power output at specific locations is strongly determined by PV power generation potential (PVpot) in the case that the installed capacity remains constant. In this study, PVpot is expressed as a dimensionless value, representing the solar energy that can be harnessed using PV cells at that specific location. It takes into account the local meteorological conditions and, as a result, is closely tied to the specific climate characteristics of the site.

At any given time t, PVpot(t) is determined by evaluating two essential aspects: (a) the actual energy production derived from the current weather condition, which includes factors like wind, temperature, and solar radiation (Radziemska, 2003), and (b) the energy production that would have been achievable under standardized test weather conditions. PVpot (t) can be computed as follows (Bichet et al., 2019; Jerez et al., 2015; Mavromatakis et al., 2010):

$$\mathrm{PV}_{\mathrm{pot}}(t) = P_R(t)\,\frac{\mathrm{RSDS}(t)}{\mathrm{RSDS}_{\mathrm{STC}}} \tag{1}$$

STC refers to standard test conditions ($\mathrm{RSDS}_{\mathrm{STC}}$ = 1,000 W/m^2), which are the conditions used to determine the nominal capacity of a PV device based on its measured power output (Bichet et al., 2019). On the other hand, P_R represents the performance ratio, which is designed to consider variations in the efficiency of PV cells caused by changes in their temperature. It can be expressed as follows:

$$P_R(t) = 1 + \gamma[T_{\mathrm{cell}}(t) - T_{\mathrm{STC}}] \tag{2}$$

The temperature of the PV cell (T_{cell}) is calculated by considering the influences of ambient temperature (TAS), solar radiation (RSDS), and wind speed (V). The standard cell temperature (T_{STC}) is taken as 25°C, and the coefficient γ is considered as 0.005°C^{-1}, based on the typical response of monocrystalline silicon solar panels (Tonui & Tripanagnostopoulos, 2008). T_{cell} can be calculated as follows (Text S1 in Supporting Information S1):

$$T_{\mathrm{cell}}(t) = c_1 + c_2\mathrm{TAS}(t) + c_3\mathrm{RSDS}(t) + c_4V(t) \tag{3}$$

with the coefficients $c_1 = 4.3$°C, $c_2 = 0.943$, $c_3 = 0.028$°C m^2 W^{-1}, and $c_4 = -1.528$°C s m^{-1} (Chenni et al., 2007). These coefficients represent the influence of meteorological conditions on cell temperature: ambient temperature determines the base temperature of the cell, strong solar radiation increases the cell temperature, and wind speed decreases the cell temperature. These coefficients are found to be fairly independent of site location and cell technology type, and have been widely used to predict PV cell temperature (Jerez et al., 2015; Feron et al., 2021).

2.3. Changes in PVpot Induced by Temperature, Radiation, and Wind

After combining Equations 1–3, the expression of PVpot can be reformulated as follows:

$$PV_{pot} = \alpha_1 RSDS + \alpha_2 RSDS^2 + \alpha_3 RSDS \cdot TAS + \alpha_4 RSDS \cdot V \quad (4)$$

where the coefficients given as $\alpha_1 = 1.1035 \times 10^{-3}$, $\alpha_2 = -1.4 \times 10^{-7}$, $\alpha_3 = -4.715 \times 10^{-6}$, and $\alpha_4 = 7.64 \times 10^{-6}$, and the changes in PVpot can be calculated using the following equation:

$$\Delta PV_{pot} = \Delta RSDS(\alpha_1 + \alpha_2 \Delta RSDS + 2\alpha_2 RSDS + \alpha_3 TAS + \alpha_4 V) + \alpha_3 RSDS \cdot \Delta TAS + \alpha_4 RSDS \cdot \Delta V + \alpha_3 \Delta RSDS \cdot \Delta TAS + \alpha_4 \Delta RSDS \cdot \Delta V \quad (5)$$

Therefore, by setting ΔTAS, ΔRSDS, or ΔV to 0, respectively, in Equation 5, the change in PVpot resulting from variations in ambient temperature, radiation and wind speed can be individually assessed. This approach has also been adopted many previous studies (Crook et al., 2011; Panagea et al., 2014; Wild et al., 2015).

2.4. Computing the Wind Power Density

Wind Power Density (WPD, W m^{-2}) serves as a parameter to evaluate the potential of wind energy (Pryor & Barthelmie, 2011). This metric is directly proportional to the cube of the wind speed at the wind turbine hub height.

$$WPD = \frac{1}{2}\rho {W_h}^3 \quad (6)$$

where ρ stands for air density, assumed to be a constant value of 1.213 kg m^{-3} under standard atmospheric conditions, while W_h represents the instantaneous wind speed at the wind turbine hub height of 100 m.

Because W_h (wind speed at the 100-m hub height of the wind turbine) is usually not directly available from climate model outputs, we follow the approach of previous studies (Lima et al., 2021; Moemken et al., 2018; Pryor et al., 2020) to extrapolate W_h using the wind power law based on the 10-m wind speed (W) obtained from the model outputs:

$$W_z = W_r \left(\frac{z}{z_r}\right)^{\alpha} \quad (7)$$

where W_r represents the wind speed at the reference height (z_r), and α is typically approximated as 1/7 (Akinsanola et al., 2021; Carvalho et al., 2021; Panagea et al., 2014).

3. Results

3.1. Impact of Aerosol Reductions on Meteorological Factors Under Carbon Neutrality

Under the carbon neutrality scenario, the concerted efforts to reduce anthropogenic emissions of aerosols and precursors yield substantial decline in AOD across China, with eastern China experiencing the most pronounced decrease. In this region, the reduction in AOD reaches values ranging from 0.1 to 0.15, approximately equating to a reduction of 30%–40% relative to the present-day level in year 2060 (Figure S1 in Supporting Information S1). It emphasizes the significant influence of the carbon neutrality initiative on aerosol loadings within China, particularly in the eastern part of the country.

Aerosols, through their interactions with radiation and clouds, have the capacity to perturb the Earth's radiation balance and thereby exert an influence on climate. Fewer aerosol particles allow more solar radiation penetrating

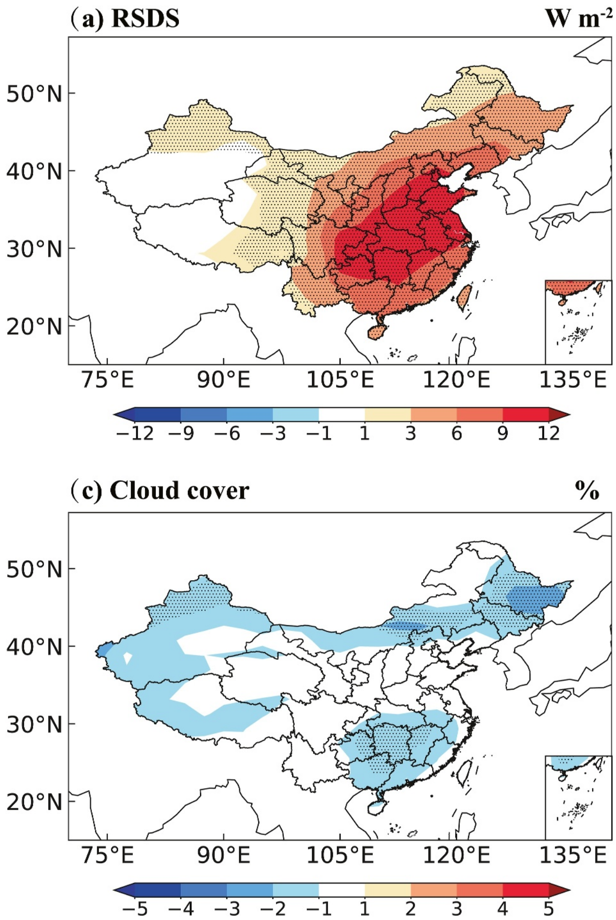

Figure 1. Spatial distribution of changes in annual mean downwelling shortwave radiation at the surface (RSDS, W m^{-2}), surface air temperature (TS, K), total cloud fraction (cloud cover, %) and wind speed (U, m s^{-1}) in 2060 under the carbon neutrality scenario in China compared to the present-day condition. The stippled areas indicate statistically significant differences at the 95% confidence level based on a two-tailed Student's *t* test.

the atmosphere and reaching the surface, which consequently lead to a rise in temperature. Changes in the ERF of anthropogenic aerosols through aerosol-radiation interactions (ARI) and ACI are estimated separately (as shown in Figure S2 of Supporting Information S1). These changes are displayed as the differences in net radiative fluxes in atmosphere-only experiments with only rapid adjustments included. In the Neutral experiments relative to the preindustrial conditions, the reductions in anthropogenic emissions of aerosols and precursor gases result in a significant positive change in the ERF_{ari}. The positive ERF_{ari} change is particularly pronounced over eastern China, with local values of 1–4 W m^{-2}. It is primarily attributed to the reduction in aerosols in the carbon neutral scenario, allowing more solar energy to reach the Earth's surface. Simultaneously, the reduction in aerosols can lead to a decrease in cloud droplet concentration, affecting cloud properties such as droplet size and cloud albedo. These changes in cloud properties contribute to a positive change in ERF_{aci}, especially in eastern China, with maximum ERF_{aci} changes exceeding 4 W m^{-2}. Although AOD has significantly decreased over the North China Plain, the change in ERF is little due to several factors like the presence of absorbing aerosols, the saturation effect of cloud droplet concentrations, and changes in local meteorological conditions (Kühn et al., 2014).

Figure 1 illustrates the changes in annual mean downwelling shortwave radiation at the surface, surface air temperature, wind speed and total cloud cover in China in year 2060 under the carbon neutrality scenario compared to the present-day conditions. In the carbon neutrality scenario, the substantial reduction in anthropogenic aerosol emissions and precursor gases leads to a significant increase in surface-downwelling shortwave radiation over eastern China, with values reaching as high as 12 W m^{-2}. Simultaneously, the considerable reduction in aerosols triggers a surface air temperature rise of 0.4–0.6 K by 2060, aligned with the increased downwelling shortwave radiation. It's noted that surface air temperature variations are influenced not only by

10.1029/2024GL109296

changes in downwelling shortwave radiation but also by factors such as longwave radiation, latent heat, sensible heat fluxes, and local meteorological conditions (J. F. Li et al., 2021). Moreover, as previous research has revealed (Jacobson & Kaufman, 2006), aerosols can exert an influence on wind speeds by altering surface temperatures and atmospheric dynamics. According to our simulations, under the carbon neutral scenario in the future, the reduction of aerosols is projected to increase wind speeds to some extent. This effect is particularly pronounced in eastern China, where wind speeds are expected to increase by approximately 0.02–0.06 m s^{-1}.

Because aerosol particles can also serve as cloud condensation nuclei to nucleate cloud droplets in the atmosphere, when aerosols decrease with else being equal, the number concentration of cloud droplets decreases, which may lead to a reduction in cloud cover. Through comparing the different experiments, we have found that under the carbon neutrality scenario, most regions across China experience a decline in cloud cover, with reductions ranging from approximately −1% to −4%. This indicates that changes in aerosol concentrations may have a significant impact on cloud formation and coverage, potentially affecting photovoltaic electricity generation.

3.2. Changes in Solar and Wind Energy Potentials Induced by Aerosol Reduction

Solar photovoltaic energy stands as a crucial renewable energy source in the quest to attain carbon neutrality objectives. The rich areas of photovoltaic power generation are mainly distributed in the western and northern regions in China, whereas the affluent regions for wind power generation are predominantly found in the western, northern, and coastal provinces (Figure S3a in Supporting Information S1). Based on the model experiments, we have conducted an in-depth assessment of solar photovoltaic potential related to the aerosol reduction under the carbon neutrality scenario (Figure 2a). In the context of the carbon neutrality scenario, by year 2060, the annual solar photovoltaic potential in China shows a significant increase. Particularly, there is an approximate 2%–8% enhancement, with both the absolute and percentage increases mainly occurring in eastern China (Figure 2a and Figure S3b in Supporting Information S1). This is primarily because PV potential is heavily influenced by surface downwelling shortwave radiation. In eastern China, the reduction of aerosols has led to a substantial increase in RSDS, with an enhancement of nearly 12 W/m^2. As previously discussed, PVpot is significantly influenced by meteorological factors, encompassing surface downwelling shortwave radiation, temperature, and wind speed. To gain a deeper understanding of how these variables affect changes in PVpot, we further decompose their individual contributions to changes in PVpot by fixing certain meteorological variables and varying others (Figure 2).

In general, the variations in PVpot due to aerosol reduction under the carbon neutrality scenario, compared to the reference scenario, are primarily attributed to changes in surface downwelling shortwave radiation, as shown in Figure 2b. This increase in surface radiation significantly enhances the efficiency of solar energy capture. The changes in temperature and wind speed, as shown in Figures 2c and 2d, respectively, have limited impacts on the changes in PVpot. Notably, in Tibetan Plateau, due to the snow/ice-albedo effect, the impact of TS on PVpot is stronger than that of RSDS. According to the Pvpot calculation, the TS increase negatively contributes to the PVpot over most western China. But over western part of Tibetan Plateau, the PVpot decreases primarily due to the increase in TS, which means a positive percentage contribution induced by TS.

Furthermore, we conduct an analysis focused on the seasonal variation in PVpot and its attribution to various meteorological factors resulting from aerosol reduction under the carbon neutrality scenario (shown in Figure 3 and Figure S4 in Supporting Information S1). RSDS changes show different spatial patterns in different seasons related variations in atmospheric circulation patterns and seasonal changes in solar radiation and cloud distributions. The variations in PVpot present different seasonally patterns. For example, during the winter season, PVpot is shown to experience an average increase exceeding 8% mostly in southwestern China. During the spring and summer seasons, the most substantial PVpot increases are expected in the eastern China, with a rise of up to 4%–8%. In autumn, the highest expected increases in PVpot are projected to occur in the North China Plain, with increases reaching up to 6%–8%. Overall, the spatial variations in PVpot during different seasons are primarily associated with the seasonal changes in downwelling shortwave radiation at the surface related to the aerosol reduction. Photovoltaic generators can be strategically placed in different locations based on seasonal data, optimizing placement and enhancing overall electricity generation efficiency.

The impact of aerosol reduction toward carbon neutrality in China on the wind power is also analyzed and shown in Figure 4a. Under the carbon-neutral emission reduction scenario, the primary changes in WPD are expected to occur in eastern China. Relative to the reference scenario, by year 2060, WPD is projected to increase by 4%–8%

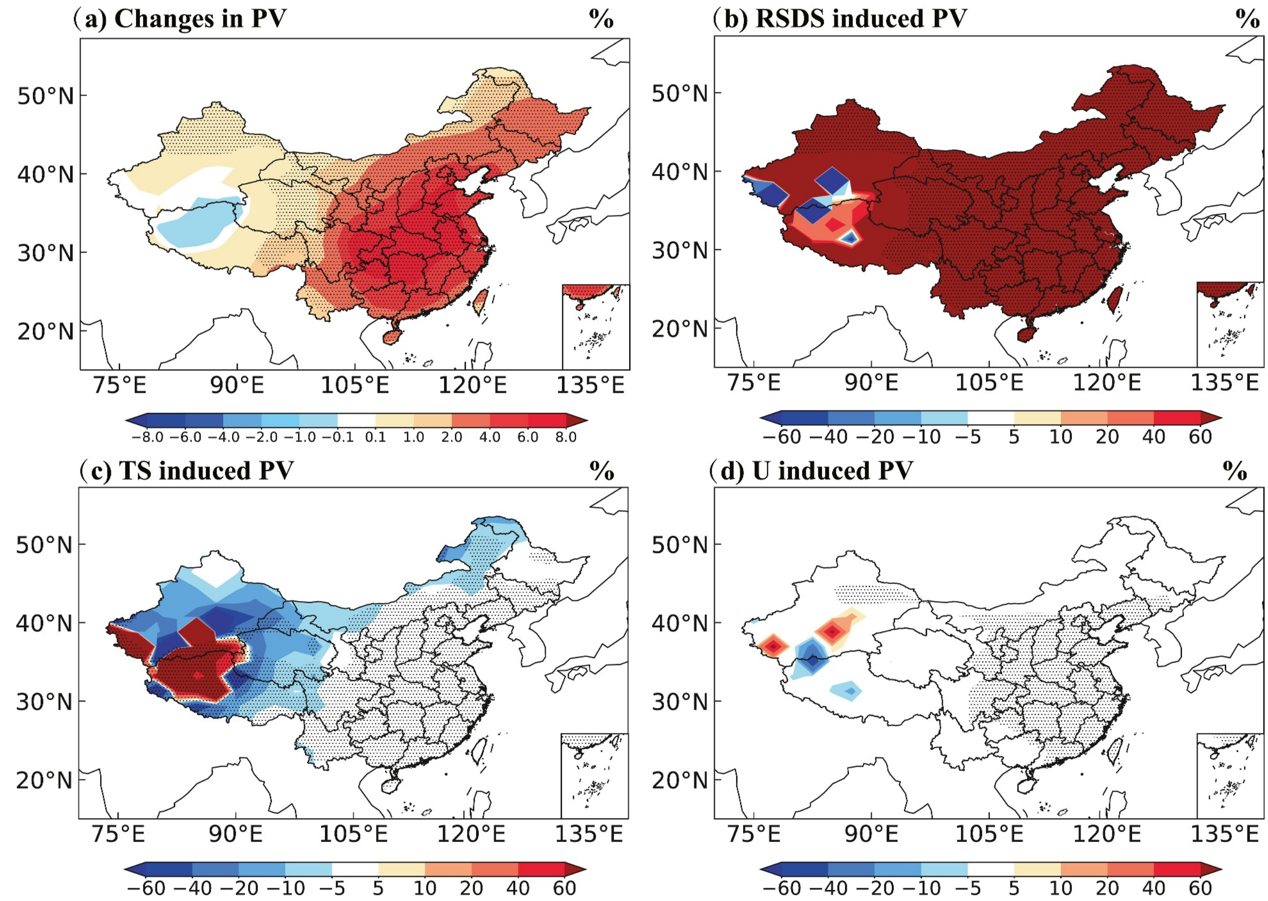

Figure 2. (a) Spatial distribution of relative changes in annual mean solar photovoltaic (PV, %) in 2060 under the carbon neutrality scenario in China compared to the present-day condition, and the PV changes contributed relatively by changes in the (b) downwelling shortwave radiation at the surface (RSDS), (c) surface air temperature (TS), and (d) the surface wind speed (U) in percentage. The stippled areas indicate statistically significant differences at the 95% confidence level based on a two-tailed Student's *t* test.

in this region. These changes are closely associated with the aerosol reduction resulting from carbon-neutral policies, primarily located in eastern China where local emissions reductions are the most significant.

Additionally, it is important to note that the variations in WPD are mainly driven by changes in wind speeds, as outlined in Equation 6 in the methodology. We further illustrate the changes in wind speeds at the 100-m height due to the future aerosol reduction under carbon neutral in 2060 (as shown in Figure 4b). In both the eastern coastal areas and eastern China, wind speeds exhibit noticeable increases, with the maximum increases reaching up to 0.06 m/s (Jacobson & Kaufman, 2006). Furthermore, the spatial patterns of wind speed changes closely resemble the response of WPD. It is worth mentioning that WPD in this study are based on wind turbines positioned at a height of 100 m above the ground level. Variations in wind speeds at different heights may yield different results. Nevertheless, our findings indicate that, under the carbon-neutral scenario, the expected increase in wind speeds due to reduced aerosol emissions is likely to lead to an enhancement in wind energy resources in China.

4. Discussions and Conclusions

In this study, the potential impacts of future aerosol reductions because of achieving carbon neutrality on solar and wind energy in China are investigated using fully coupled climate model (CESM1) experiments. Under the carbon neutral scenario, there are significant reductions in emissions of aerosols and precursors, particularly in eastern China, where AOD decreases by approximately 30%–40%. By year 2060, due to the aerosol reduction

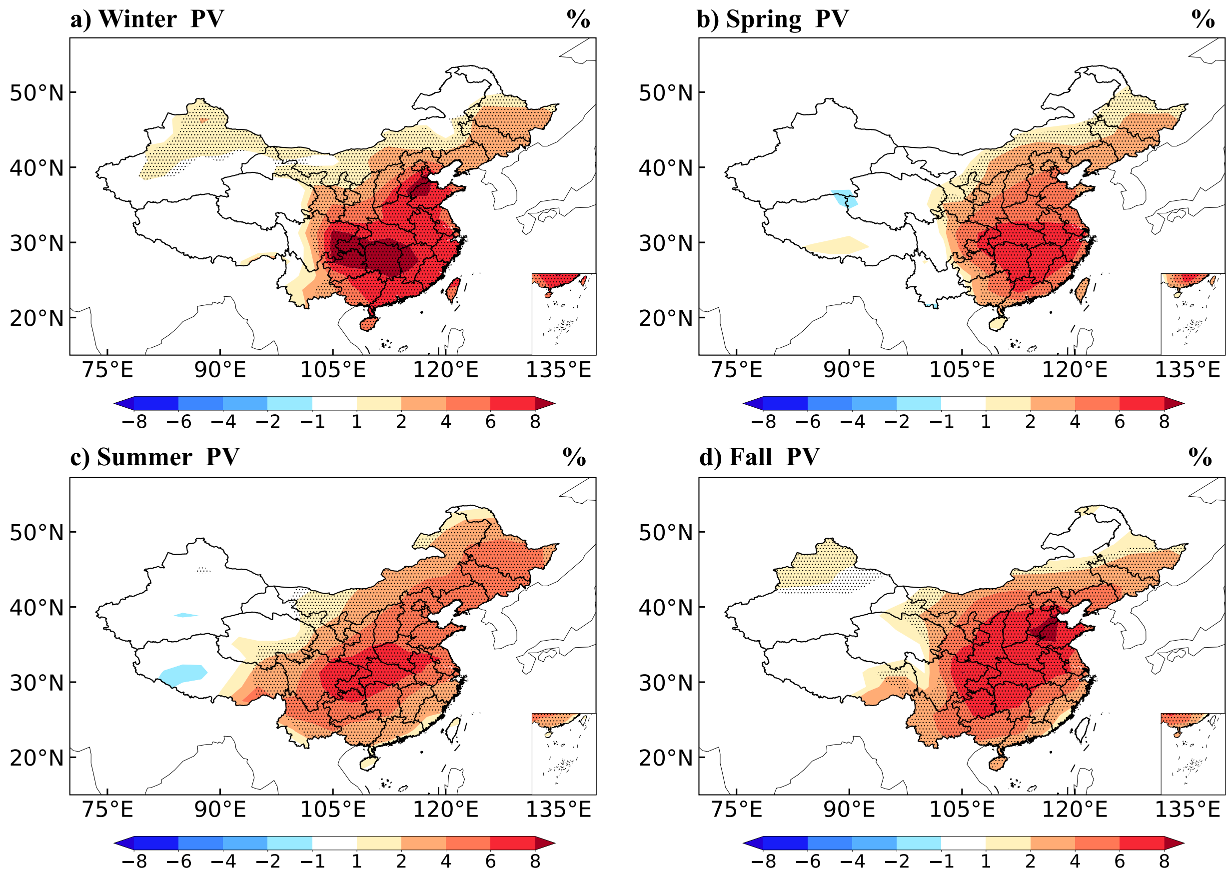

Figure 3. Spatial distribution of relative changes in annual mean solar photovoltaic (%) in 2060 under the carbon neutrality scenario in China compared to the present-day condition as averaged in (a) December–January–February (Winter), (b) March–April–May (Spring), (c) July–August (Summer), and (d) September–October–November (Fall). The stippled areas indicate statistically significant differences at the 95% confidence level based on a two-tailed Student's *t* test.

under the carbon neutrality scenario, most regions in China are shown to experience a significant increase in downwelling shortwave radiation at the surface and surface air temperatures, with values reaching as high as 12 W m^{-2} in the eastern region and a temperature rise of 0.4–0.6 K. Additionally, the reduction in aerosols is expected to increase wind speeds, especially in eastern China, with an estimated increase of 0.02–0.06 m s^{-1}.

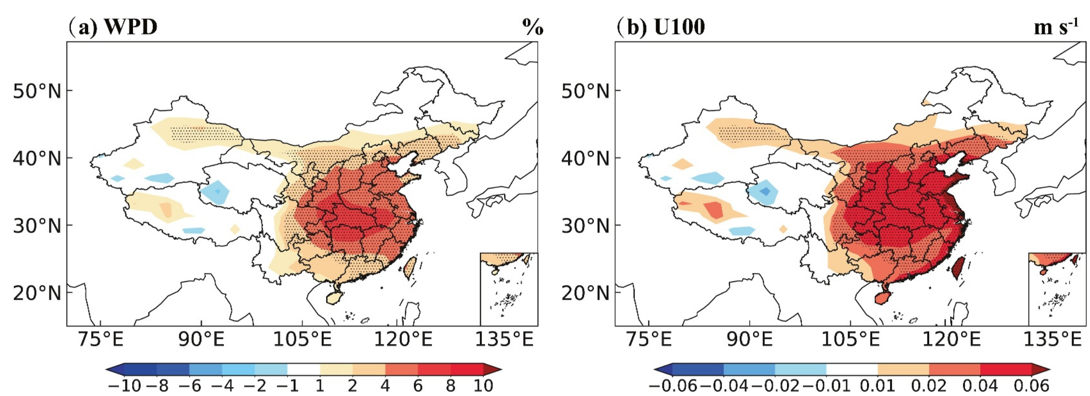

Figure 4. Spatial distribution of relative changes in annual mean Wind Power Density (WPD, %) and wind speed at a height of 100 m (U100, %) in 2060 under the carbon neutrality scenario in China compared to the present-day condition. The stippled areas indicate statistically significant differences at the 95% confidence level based on a two-tailed Student's *t* test.

These findings underscore the substantial impacts of China's carbon neutrality implementation on aerosol loading and related meteorological conditions.

In the pursuit of carbon neutrality goals, solar photovoltaic and wind energy have emerged as critical renewable energy resources. A detailed assessment of PVpot in China under the carbon neutrality scenario reveals a significant increase by 2060, ranging from 2% to 8%, with the most substantial improvements occurring in the eastern region. This potential is greatly influenced by meteorological factors, with the surface downwelling shortwave radiation being the primary driver, enhancing the efficiency of solar energy capture. Although temperature and wind speed also play a role, their impacts are relatively limited. Seasonal variations in PVpot are closely linked to changes in the surface downwelling shortwave radiation. Furthermore, aerosol reductions related to the implementation of China's carbon-neutral policies lead to an increase in wind power resources in eastern China, projected to rise by 4%–8% by 2060, primarily driven by enhanced wind speeds. Spatial patterns of wind speed changes closely align with wind power responses, indicating the potential for increased wind energy resources under the carbon-neutral scenario.

This study provides a comprehensive assessment of solar photovoltaic and wind energy resources in China due to the reductions in anthropogenic emissions of aerosols and precursors under the carbon neutrality scenario. Previous studies have assessed the performance of the CESM model by comparing it with reanalysis data sets. These studies found that CESM performs well in long-term simulations, and its representation of global and regional climate states is relatively reasonable when compared to reanalysis data (Z. Wang et al., 2015). Moreover, large model uncertainties exist in projections of climate response to anthropogenic forcing, and CESM is relatively more sensitive to anthropogenic forcings. CESM generally has a higher ERF due to ACI than other climate models (Zelinka et al., 2014). However, we acknowledge the presence of certain limitations and uncertainties in this study. First, CESM1 underestimates aerosol concentrations in China (Ren et al., 2021), which could potentially result in a low bias in the simulated future climate change related to aerosol variations. Future research endeavors could adopt a multi-model approach to reduce reliance on a single model. Additionally, future clean air actions in China may also influence tropospheric ozone concentrations, which, as a greenhouse gas, could impact climate (J. Gao et al., 2022; P. Wang et al., 2023) and should be considered in future investigations using models with comprehensive gas chemistry modules. Moreover, previous research has indicated that the installation of wind turbines and solar panels can alter surface properties such as roughness and albedo, leading to regional climate changes (Y. Li et al., 2018; Zhou et al., 2012). However, our study did not consider the potential impact of constructed wind and solar installations on climate simulation. As previous studies have noted the differences in climate response between transient and stabilized scenarios (King et al., 2020), it is essential to conduct further in-depth exploration to better understand the future projections of climate change. Despite these limitations, our research findings hold significant value for informing China's long-term renewable energy investment plans. Our findings suggest that despite the adverse effects on climate warming due to aerosol reductions, certain regions in China have the potential to observe substantial co-benefits in terms of solar photovoltaic resources and wind in the context of carbon reduction and pollution control, which serves as evidence to support a faster transition to clean energy and the achievement of carbon neutrality goals.

Acknowledgments

This study was supported by the National Key Research and Development Program of China (Grant 2019YFA0606800), Jiangsu Science Fund for Distinguished Young Scholars (Grant BK20211541), the Jiangsu Science Fund for Carbon Neutrality (Grant BK20220031), Jiangsu Innovation and Entrepreneurship Team (Grant JSSCTD202346), and Open fund by Jiangsu Key Laboratory of Atmospheric Environment Monitoring and Pollution Control (Grant KHK 23002). HW acknowledges the support by the U.S. Department of Energy (DOE), Office of Science, Office of Biological and Environmental Research (BER), as part of the Earth and Environmental System Modeling program. The Pacific Northwest National Laboratory (PNNL) is operated for DOE by the Battelle Memorial Institute under contract DE-AC05-76RLO1830.

Data Availability Statement

The modeling results used in this study are available at Ren et al. (2024).

References

Akinsanola, A. A., Ogunjobi, K. O., Abolude, A. T., & Salack, S. (2021). Projected changes in wind speed and wind energy potential over West Africa in CMIP6 models. *Environmental Research Letters*, *16*(4), 044033. https://doi.org/10.1088/1748-9326/abed7a

AlSkaif, T., Dev, S., Visser, L., Hossari, M., & van Sark, W. (2020). A systematic analysis of meteorological variables for PV output power estimation. *Renewable Energy*, *153*, 12–22. https://doi.org/10.1016/j.renene.2020.01.150

Bichet, A., Hingray, B., Evin, G., Diedhiou, A., Kebe, C. M. F., & Anquetin, S. (2019). Potential impact of climate change on solar resource in Africa for photovoltaic energy: Analyses from CORDEX-AFRICA climate experiments. *Environmental Research Letters*, *14*(12), 124039. https://doi.org/10.1088/1748-9326/ab500a

Carvalho, D., Rocha, A., Costoya, X., DeCastro, M., & Gómez-Gesteira, M. (2021). Wind energy resource over Europe under CMIP6 future climate projections: What changes from CMIP5 to CMIP6. *Renewable and Sustainable Energy Reviews*, *151*, 111594. https://doi.org/10.1016/j.rser.2021.111594

Chen, L. (2020). Impacts of climate change on wind resources over North America based on NA-CORDEX. *Renewable Energy*, *153*, 1428–1438. https://doi.org/10.1016/j.renene.2020.02.090

Chen, Y., Yue, X., Tian, C., Letu, H., Wang, L., Zhou, H., et al. (2023). Assessment of solar energy potential in China using an ensemble of photovoltaic power models. *Science of the Total Environment*, *877*, 162979. https://doi.org/10.1016/j.scitotenv.2023.162979

Cheng, J., Tong, D., Liu, Y., Yu, S., Yan, L., Zheng, B., et al. (2021). Comparison of current and future $PM_{2.5}$ air quality in China under CMIP6 and DPEC emission scenarios. *Geophysical Research Letters*, *48*(11), e2021GL093197. https://doi.org/10.1029/2021GL093197

Chenni, R., Makhlouf, M., Kerbache, T., & Bouzid, A. (2007). A detailed modeling method for photovoltaic cells. *Energy*, *32*(9), 1724–1730. https://doi.org/10.1016/j.energy.2006.12.006

Crook, J. A., Jones, L. A., Forster, P. M., & Crook, R. (2011). Climate change impacts on future photovoltaic and concentrated solar power energy output. *Energy & Environmental Science*, *4*(9), 3101–3109. https://doi.org/10.1039/C1EE01495A

Feron, S., Cordero, R. R., Damiani, A., & Jackson, R. B. (2021). Climate change extremes and photovoltaic power output. *Nature Sustainability*, *4*(3), 270–276. https://doi.org/10.1038/s41893-020-00643-w

Gao, J., Yang, Y., Wang, H., Wang, P., Li, H., Li, M., et al. (2022). Fast climate responses to emission reductions in aerosol and ozone precursors in China during 2013–2017. *Atmospheric Chemistry and Physics*, *22*(11), 7131–7142. https://doi.org/10.5194/acp-22-7131-2022

Gao, M., Ding, Y., Song, S., Lu, X., Chen, X., & McElroy, M. B. (2018). Secular decrease of wind power potential in India associated with warming in the Indian Ocean. *Science Advances*, *4*(12), eaat5256. https://doi.org/10.1126/sciadv.aat5256

Ghan, S. J. (2013). Estimating aerosol effects on cloud radiative forcing. *Atmospheric Chemistry and Physics*, *13*(19), 9971–9974. https://doi.org/10.5194/acp-13-9971-2013

Huang, M.-T., & Zhai, P.-M. (2021). Achieving Paris Agreement temperature goals requires carbon neutrality by middle century with far-reaching transitions in the whole society. *Advances in Climate Change Research*, *12*(2), 281–286. https://doi.org/10.1016/j.accre.2021.03.004

Hurrell, J. W., Holland, M. M., Gent, P. R., Ghan, S., Kay, J. E., Kushner, P. J., et al. (2013). The Community Earth System Model: A Framework for Collaborative Research. *Bulletin of the American Meteorological Society*, *94*(9), 1339–1360. https://doi.org/10.1175/BAMS-D-12-00121.1

Jacobson, M. Z., & Kaufman, Y. J. (2006). Wind reduction by aerosol particles. *Geophysical Research Letters*, *33*(24), L24814. https://doi.org/10.1029/2006GL027838

Jerez, S., Tobin, I., Vautard, R., Montávez, J. P., López-Romero, J. M., Thais, F., et al. (2015). The impact of climate change on photovoltaic power generation in Europe. *Nature Communications*, *6*(1), 10014. https://doi.org/10.1038/ncomms10014

King, A. D., Lane, T. P., Henley, B. J., & Brown, J. R. (2020). Global and regional impacts differ between transient and equilibrium warmer worlds. *Nature Climate Change*, *10*(1), 42–47. https://doi.org/10.1038/s41558-019-0658-7

Kühn, T., Partanen, A. I., Laakso, A., Lu, Z., Bergman, T., Mikkonen, S., et al. (2014). Climate impacts of changing aerosol emissions since 1996. *Geophysical Research Letters*, *41*(13), 4711–4718. https://doi.org/10.1002/2014GL060349

Lei, Y., Wang, Z., Wang, D., Zhang, X., Che, H., Yue, X., et al. (2023). Co-benefits of carbon neutrality in enhancing and stabilizing solar and wind energy. *Nature Climate Change*, *13*(7), 693–700. https://doi.org/10.1038/s41558-023-01692-7

Li, J. F., Xu, K. M., Lee, W. L., Jiang, J. H., Fetzer, E., Yu, J. Y., et al. (2021). Linking global land surface temperature projections to radiative effects of hydrometeors under a global warming scenario. *Environmental Research Letters*, *16*(8), 084044. https://doi.org/10.1088/1748-9326/ac153c

Li, Y., Kalnay, E., Motesharrei, S., Rivas, J., Kucharski, F., Kirk-Davidoff, D., et al. (2018). Climate model shows large-scale wind and solar farms in the Sahara increase rain and vegetation. *Science*, *361*(6406), 1019–1022. https://doi.org/10.1126/science.aar5629

Lima, D. C., Soares, P. M., Cardoso, R. M., Semedo, A., Cabos, W., & Sein, D. V. (2021). The present and future offshore wind resource in the Southwestern African region. *Climate Dynamics*, *56*(5–6), 1371–1388. https://doi.org/10.1007/s00382-020-05536-4

Liu, X., Ma, P. L., Wang, H., Tilmes, S., Singh, B., Easter, R. C., et al. (2016). Description and evaluation of a new four-mode version of the Modal Aerosol Module (MAM4) within version 5.3 of the Community Atmosphere Model. *Geoscientific Model Development*, *9*(2), 505–522. https://doi.org/10.5194/gmd-9-505-2016

Liu, Z., Deng, Z., He, G., Wang, H., Zhang, X., Lin, J., et al. (2022). Challenges and opportunities for carbon neutrality in China. *Nature Reviews Earth & Environment*, *3*(2), 141–155. https://doi.org/10.1038/s43017-021-00244-x

Mavromatakis, F., Makrides, G., Georghiou, G., Pothrakis, A., Franghiadakis, Y., Drakakis, E., & Koudoumas, E. (2010). Modeling the photovoltaic potential of a site. *Renewable Energy*, *35*(7), 1387–1390. https://doi.org/10.1016/j.renene.2009.11.010

Moemken, J., Reyers, M., Feldmann, H., & Pinto, J. G. (2018). Future changes of wind speed and wind energy potentials in EURO-CORDEX ensemble simulations. *Journal of Geophysical Research: Atmospheres*, *123*(12), 6373–6389. https://doi.org/10.1029/2018JD028473

Panagea, I. S., Tsanis, I. K., Koutroulis, A. G., & Grillakis, M. G. (2014). Climate change impact on photovoltaic energy output: The case of Greece. *Advances in Meteorology*, *2014*, 1–11. https://doi.org/10.1155/2014/264506

Park, C., Shin, S. W., Kim, G., Cha, D. H., Min, S. K., Lee, D., et al. (2022). What determines future changes in photovoltaic potential over East Asia? *Renewable Energy*, *185*, 338–347. https://doi.org/10.1016/j.renene.2021.12.029

Pryor, S., & Barthelmie, R. (2011). Assessing climate change impacts on the near-term stability of the wind energy resource over the United States. *Proceedings of the National Academy of Sciences*, *108*(20), 8167–8171. https://doi.org/10.1073/pnas.1019388108

Pryor, S. C., Barthelmie, R. J., Bukovsky, M. S., Leung, L. R., & Sakaguchi, K. (2020). Climate change impacts on wind power generation. *Nature Reviews Earth & Environment*, *1*(12), 627–643. https://doi.org/10.1038/s43017-020-0101-7

Radziemska, E. (2003). The effect of temperature on the power drop in crystalline silicon solar cells. *Renewable Energy*, *28*, 1–12. https://doi.org/10.1016/S0960-1481(02)00015-0

Ren, L., Yang, Y., Wang, H., Wang, P., Chen, L., Zhu, J., & Liao, H. (2021). Aerosol transport pathways and source attribution in China during the COVID-19 outbreak. *Atmospheric Chemistry and Physics*, *21*(20), 15431–15445. https://doi.org/10.5194/acp-21-15431-2021

Ren, L., Yang, Y., Wang, H., Wang, P., Yue, X., & Liao, H. (2022). Widespread wildfires over the western United States in 2020 linked to emissions reductions during COVID-19. *Geophysical Research Letters*, *49*(15), e2022GL099308. https://doi.org/10.1029/2022GL099308

Ren, L., Yang, Y., Wang, H., Wang, P., Yue, X., & Liao, H. (2024). Co-benefits of mitigating aerosol pollution to future solar and wind energy in China toward carbon neutrality [Dataset]. *Zenodo*. https://doi.org/10.5281/zenodo.6482166

Rogelj, J., Geden, O., Cowie, A., & Reisinger, A. (2021). Three ways to improve net-zero emissions targets. *Nature*, *591*(7850), 365–368. https://doi.org/10.1038/d41586-021-00662-3

Sailor, D. J., Smith, M., & Hart, M. (2008). Climate change implications for wind power resources in the Northwest United States. *Renewable Energy*, *33*(11), 2393–2406. https://doi.org/10.1016/j.renene.2008.01.007

Shindell, D., & Smith, C. J. (2019). Climate and air-quality benefits of a realistic phase-out of fossil fuels. *Nature*, *573*(7774), 408–411. https://doi.org/10.1038/s41586-019-1554-z

Tong, D., Cheng, J., Liu, Y., Yu, S., Yan, L., Hong, C., et al. (2020). Dynamic projection of anthropogenic emissions in China: Methodology and 2015–2050 emission pathways under a range of socio-economic, climate policy, and pollution control scenarios. *Atmospheric Chemistry and Physics*, *20*(9), 5729–5757. https://doi.org/10.5194/acp-20-5729-2020

Tonui, J. K., & Tripanagnostopoulos, Y. (2008). Performance improvement of PV/T solar collectors with natural air flow operation. *Solar Energy*, *82*, 1–12. https://doi.org/10.1016/j.solener.2007.06.004

Wang, H., Easter, R. C., Rasch, P. J., Wang, M., Liu, X., Ghan, S. J., et al. (2013). Sensitivity of remote aerosol distributions to representation of cloud–aerosol interactions in a global climate model. *Geoscientific Model Development*, *6*(3), 765–782. https://doi.org/10.5194/gmd-6-765-2013

Wang, P., Yang, Y., Xue, D., Ren, L., Tang, J., Leung, L. R., & Liao, H. (2023). Aerosols overtake greenhouse gases causing a warmer climate and more weather extremes toward carbon neutrality. *Nature Communications*, *14*(1), 7257. https://doi.org/10.1038/s41467-023-42891-2

Wang, Z., Li, Y., Liu, B., & Liu, J. (2015). Global climate internal variability in a 2000-year control simulation with Community Earth System Model (CESM). *Chinese Geographical Science*, *25*(3), 263–273. https://doi.org/10.1007/s11769-015-0754-1

Wild, M., Folini, D., Henschel, F., Fischer, N., & Müller, B. (2015). Projections of long-term changes in solar radiation based on CMIP5 climate models and their influence on energy yields of photovoltaic systems. *Solar Energy*, *116*, 12–24. https://doi.org/10.1016/j.solener.2015.03.039

Yang, H., Huang, X., Hu, J., Thompson, J. R., & Flower, R. J. (2022). Achievements, challenges and global implications of China's carbon neutral pledge. *Frontiers of Environmental Science & Engineering*, *16*(8), 111. https://doi.org/10.1007/s11783-022-1532-9

Yang, Y., Ren, L., Li, H., Wang, H., Wang, P., Chen, L., et al. (2020). Fast climate responses to aerosol emission reductions during the COVID-19 pandemic. *Geophysical Research Letters*, *47*(19), e2020GL089788. https://doi.org/10.1029/2020GL089788

Yang, Y., Zeng, L., Wang, H., Wang, P., & Liao, H. (2023). Climate effects of future aerosol reductions for achieving carbon neutrality in China. *Science Bulletin*, *68*(9), 902–905. https://doi.org/10.1016/j.scib.2023.03.048

Zelinka, M. D., Andrews, T., Forster, P. M., & Taylor, K. E. (2014). Quantifying components of aerosol-cloud-radiation interactions in climate models. *Journal of Geophysical Research: Atmospheres*, *119*(12), 7599–7615. https://doi.org/10.1002/2014JD021710

Zhao, W. (2022). China's goal of achieving carbon neutrality before 2060: Experts explain how. *National Science Review*, *9*(8), nwac115. https://doi.org/10.1093/nsr/nwac115

Zhou, L., Tian, Y., Baidya Roy, S., Thorncroft, C., Bosart, L. F., & Hu, Y. (2012). Impacts of wind farms on land surface temperature. *Nature Climate Change*, *2*(7), 539–543. https://doi.org/10.1038/nclimate1505